Cancer Diagnostics

International Edition: DOI: 10.1002/anie.201502899
German Edition: DOI: 10.1002/ange.201502899

Fluorescent In Situ Targeting Probes for Rapid Imaging of Ovarian-Cancer-Specific γ-Glutamyltranspeptidase**

Feiyi Wang, Ying Zhu, Li Zhou, Liang Pan, Zhifen Cui, Qiang Fei, Sihang Luo, Dun Pan, Qing Huang†, Rui Wang, Chunchang Zhao, He Tian, and Chunhai Fan**

In memory of Qing Huang

Abstract: *γ-Glutamyltranspeptidase (GGT) is a tumor biomarker that selectively catalyzes the cleavage of glutamate overexpressed on the plasma membrane of tumor cells. Here, we developed two novel fluorescent in situ targeting (FIST) probes that specifically target GGT in tumor cells, which comprise 1) a GGT-specific substrate unit (GSH), and 2) a boron–dipyrromethene (BODIPY) moiety for fluorescent signalling. In the presence of GGT, sulfur-substituted BODIPY was converted to amino-substituted BODIPY, resulting in dramatic fluorescence variations. By exploiting this enzyme-triggered photophysical property, we employed these FIST probes to monitor the GGT activity in living cells, which showed remarkable differentiation between ovarian cancer cells and normal cells. These probes represent two first-generation chemodosimeters featuring enzyme-mediated rapid, irreversible aromatic hydrocarbon transfer between the sulfur and nitrogen atoms accompanied by switching of photophysical properties.*

The challenges in rapid and accurate localization of malignant cancers promote the development of analytical techniques for highly sensitive detection and analysis of cancer-related biomarkers. Particularly, clinical measurement of cancer-related biomarkers holds great potential for rapid prediction for cancer diagnosis, treatment, and management.[1,2] Among many potential targets, enzymes are gaining intense attention as a promising class of biomarkers because of their chemical specificity and rapid catalytic reactions, which makes biological events of interest to be rapidly and selectively identified.[3–23] GGT is a cell membrane-bound enzyme, which selectively catalyzes the cleavage of the γ-glutamyl bond in GSH, resulting in the production of cysteinyl-glycine, followed by formation of cysteine and glycine induced by plasma membrane dipeptidase.[24] As malignant cells are highly dependent on cysteine, GGT-mediated metabolism of extracellular GSH confers growth and survival advantages for tumor cells. Indeed, it has been discovered that overexpressed levels of GGT are associated with tumorigenesis in several human cancer cells, as represent by cervical and ovarian cancers.[25–27] Thus, GGT can be regarded as a biomarker for cancer diagnosis as well as a therapeutic target.

GGT assays have attracted intense interest. *p*-Nitroanilide-based colorimetric assay is a conventional way to monitor GGT activity,[28] which nevertheless is not compatible with real-time imaging in living cells. Fluorescence imaging using a fluorescent probe has been widely recognized as a non-invasive and real-time approach for detection of the targets of interest in vitro or in vivo. An aminomethylcoumarin-based fluorescent probe was previously developed for GGT imaging, which nevertheless has not been exploited for in vivo imaging because of its high fluorescence background and poor sensitivity.[29] Recently, Urano et al. reported an activated fluorescent probe for in vitro or in vivo imaging of GGT.[16] However, this probe adopts a fluorescence turn-on mode that is susceptible to experimental conditions. We reason that ratiometric probes endowing a self-calibration effect can greatly eliminate interferences including dye concentration, microenvironments, instrumental efficiency, and photobleaching, which motivated us to develop more reliable and versatile probes. In this contribution, we focused on the design of FIST probes using γ-glutamyltranspeptidase

[*] F. Wang,[+] Q. Fei, S. Luo, Prof. C. Zhao, Prof. H. Tian
Key Laboratory for Advanced Materials and
Institute of Fine Chemicals
East China University of Science & Technology
Shanghai 200237 (China)
E-mail: zhaocchang@ecust.edu.cn
Prof. Y. Zhu,[+] L. Pan, Z. Cui, Dr. D. Pan, Prof. Q. Huang, Prof. C. Fan
Division of Physical Biology & Bioimaging Center
Shanghai Synchrotron Radiation Facility
CAS Key Laboratory of Interfacial Physics and Technology
Shanghai Institute of Applied Physics, Chinese Academy of Sciences
Shanghai 201800 (China)
E-mail: fchh@sinap.ac.cn
L. Zhou, Prof. R. Wang
Shanghai Key Laboratory of New Drug Design
School of Pharmacy
East China University of Science & Technology
Shanghai 200237 (P. R. China)
[+] These authors contributed equally to this work.
[†] Deceased.
[**] We gratefully acknowledge the financial support by the National Science Foundation of China (grant numbers 21172071, 21190033, 21372083, 21375139, 21390414, and 91313302), and the Ministry of Science and Technology (grant numbers 2013CB933802 and 2012CB825805).
Supporting information for this article is available on the WWW under http://dx.doi.org/10.1002/anie.201502899.

(GGT) as an imaging target for real-time detection of cancer cells. We directly conjugated GSH to a fluorophore to construct an enzyme-switching probe. We envisioned that development of such a fluorophore-GSH adduct as a GGT-triggered probe should provide invaluable insights into how GGT works in complex biological systems, and eventually afford specific, rapid, and accurate detection of GGT-related cancer cells, such as ovarian cancers.

We first designed two GGT-specific fluorescent probes, **M-BODIPY-GSH** and **C-BODIPY-GSH** (Scheme 1) capable of specific monitoring GGT activity. In our design, these probes have GSH moiety as the substrate to target GGT, with the free thiol function covalently attached to the BODIPY scaffold. Upon GGT enzymatic cleavage of γ-glutamyl linkage, the released amino group in cysteinylglycine residue then undergoes intramolecular displacement of thiolate to yield amino-substituted **BODIPY-Cys** adduct through five-membered cyclic transition state, which exhibits dramatically different photophysical properties compared with the sulfur-substituted **M-BODIPY-GSH** or **C-BODIPY-GSH**. This enables the visualization of GGT activities in living cells. **M-BODIPY-GSH** and **C-BODIPY-GSH** represent two first-generation chemodosimeters featuring enzyme-mediated, rapid, irreversible aromatic hydrocarbon transfer between the sulfur and nitrogen atoms accompanied with the switching of photophysical properties. According to the design strategy here, by replacing the γ-glutamyl group of the peptide-based substrate with a suitable moiety, novel enzyme-activatable probes could be constructed.

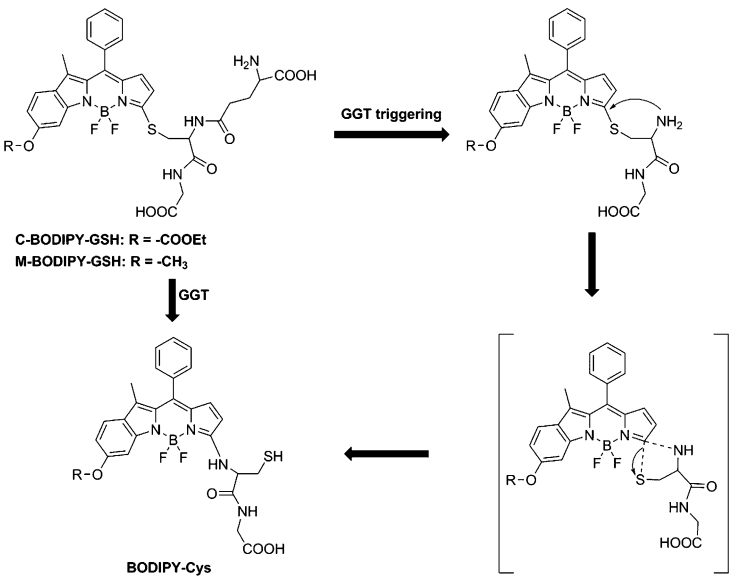

Scheme 1. Proposed mechanism of GGT triggering fluorescence change of **M-BODIPY-GSH** or **C- BODIPY-GSH**.

The synthesis of **M-BODIPY-GSH** or **C-BODIPY-GSH** was simply achieved by nucleophilic aromatic substitution (S_NAr) of the chlorine of monochlorinated BODIPY derivative with free thiol group on GSH (see Scheme S1 in the Supporting Information).[30] The purity and identity were verified by high-resolution mass spectrometry (HRMS), ^1H NMR and ^{13}C NMR spectroscopy.

To establish that our newly designed **M-BODIPY-GSH** and **C-BODIPY-GSH** are indeed promising fluorescent probes capable of GGT activity assay, the photophysical properties in the absence and presence of GGT were explored in phosphate-buffered saline (PBS) solution (pH 7.4). As shown in Figure 1 and Table S1, the two probes showed dramatic optical response to GGT in vitro. In the absence of GGT, an intense absorption at 578 nm and a relatively weak emission band at 601 nm were observed for **M-BODIPY-GSH**. Upon incubation with GGT, the absorption and fluorescence spectra showed time-dependent features. As the incubation time proceeded, the absorption band at 578 nm was reduced and a new band at 510 nm was built up concomitantly, with an obvious isosbestic point at 528 nm. In the fluorescence spectra, the emission maximum underwent a hypochromic shift from 601 to 582 nm accompanied by a remarkable fluorescence enhancement. Both the emission intensity at 582 nm and the intensity ratio, I_{582}/I_{601}, (Figure S1), increased within the time course of 20 minutes and reached a plateau at this time point, which allow the rapid assay of GGT activity by both ratiometric and normal turn-on fluorescence methods. However, minimal fluorescence enhancement was observed by pretreatment of GGT with acivicin (Figure S2), a broad-spectrum inhibitor of GGT,[31] confirming the essential role of GGT in triggering the fluorescence signal change. These observed optical responses could be attributed to the cleavage of γ-glutamyl linkage to

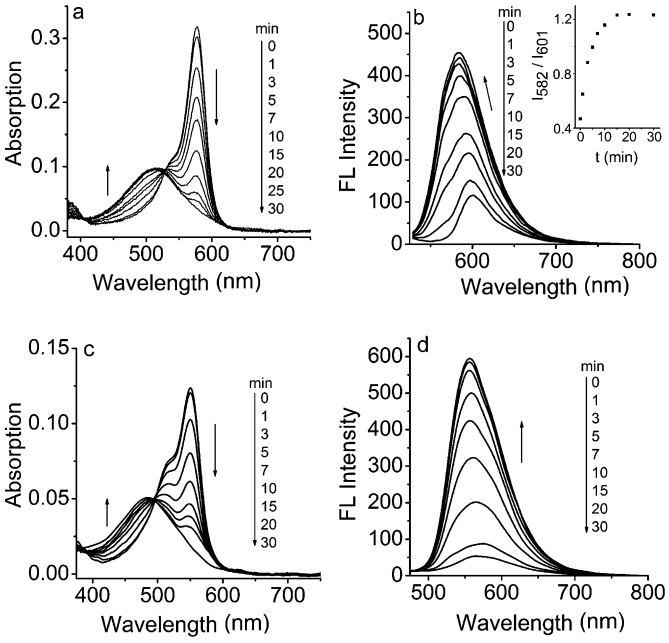

Figure 1. Time-dependent spectra changes of **M-BODIPY-GSH** and **C-BODIPY-GSH** (10 μM) in the presence of GGT (30 mU mL^{-1}) in PBS buffer (pH 7.4) at 37 °C. **M-BODIPY-GSH**: a) Absorption, b) emission (λ_{ex} = 510 nm), inset is the ratiometric fluorescence intensity changes of **M-BODIPY-GSH** upon enzymatic reaction with GGT; **C-BODIPY-GSH**: c) Absorption, d) emission (λ_{ex} = 450 nm).

liberate free amino function, followed by an intramolecular displacement of thiolate to yield an amino-substituted **BODIPY-Cys** adduct by a five-membered cyclic transition state (Scheme 1). This translation between the sulfur and nitrogen atoms is consistent with the reaction mechanism between monochlorinated BODIPY and cysteine, which have been demonstrated to undergo the same intramolecular rearrangement to produce amino-substituted BODIPY, reported by our and Yang's group.[32,33] Thus, the photophysical properties of **BODIPY-Cys** match well with that of monochlorinated BODIPY + cysteine (Figure S3). The production of **BODIPY-Cys** was also identified by the HRMS analysis. The mixture of **M-BODIPY-GSH** and GGT manifested a mass peak at 539.1754 identical to [**BODIPY-Cys**]$^+$ (Figure S4). The incubation of **C-BODIPY-GSH** with GGT resulted in the same reaction as observed for **M-BODIPY-GSH**. Noteworthy, **C-BODIPY-GSH** gave a fluorescence turn-on response with a higher signal to background ratio than **M-BODIPY-GSH**, thus enabling **C-BODIPY-GSH** especially favorable for in vivo imaging.

To obtain the optimal amount of GGT and **M-BODIPY-GSH** or **C-BODIPY-GSH** explored in the assay, the titration experiments of the enzymatic reaction between GGT and the two probes were monitored (Figure S5). With the increase of GGT concentrations from 0 to 30 mU mL^{-1}, the fluorescence intensity of **M-BODIPY-GSH** (10 μM) is progressively intensified. Further addition resulted in no more change, suggesting that 30 mU mL^{-1} GGT can catalyze the metabolism of 10 μM **M-BODIPY-GSH**. Likely, when GGT (30 mU mL^{-1}) is treated with various concentrations of **M-BODIPY-GSH**, a dose-dependent fluorescence increase was observed. These experimental data once again demonstrated that 10 μM **M-BODIPY-GSH** is sufficient for digestion by 30 mU mL^{-1} GGT. Similar results were observed for **C-BODIPY-GSH**. The kinetic values of the two probes against GGT were further determined according to Michaelis–Menten equation, and the K_m and V_{max} values were 18.70 μM and 3.65 μM min^{-1} for **M-BODIPY-GSH**, 18.76 μM and 3.38 μM min^{-1} for **C-BODIPY-GSH**, respectively (Figure S6).

M-BODIPY-GSH and **C-BODIPY-GSH** unambiguously exhibited high specificity for GGT activity (Figure 2). Treatment with other proteins, such as collagen hydrolase, phosphatase, aprotinin, and glucoamylase, induced no observable fluorescence change. The stability of both probes was also examined in PBS buffer solution containing 10% FBS or 10% human Plasma. Negligible hydrolyzation under these conditions was found, indicative of the specific recognition and cleavage by GGT. The experiments for interrogating effects of some important metal ions on the response process were also investigated, which demonstrated that these metal ions have little influence on the response properties (Figure S7).

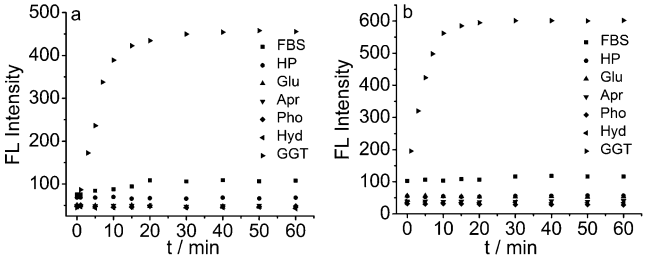

Figure 2. Stability of a) **M-BODIPY-GSH** (10 μM) and b) **C-BODIPY-GSH** (10 μM) in PBS buffer solution toward different substrates, which include 10% FBS, 10% human plasma, collagen hydrolase, phosphatase, aprotinin, and glucoamylase. The fluorescence intensity at 582 nm for **M-BODIPY-GSH** and 556 nm for **C-BODIPY-GSH** were selected for the stability discussion.

Inspired by the demonstration of the use of **M-BODIPY-GSH** and **C-BODIPY-GSH** for specific monitoring the GGT activity, we next examined the capability of the FIST probes for evaluation of GGT activity in living cancer cells. Since **M-BODIPY-GSH** can serve as a ratiometric fluorescence probe for monitoring GGT, we investigated the feasibility of this probe to detect ovarian cancer cells in a dual-color manner (Figure 3 and Figure S8). When human ovarian cancer cells, OVCAR5 cells, were incubated with **M-BODIPY-GSH** (10 μM) for 30 minutes, bright fluorescence signals in the yellow channel (554–584 nm) were collected. In contrast, relatively low fluorescence signals were observed in the red channel (595–635 nm). The ratio of the two emissions generated from yellow channel to red channel is about 1.4. Other ovarian cancer cells, such as SKOV3 cells showed the similar imaging pattern (Figure 3 and Figure S8). In comparison, when normal cells, human umbilical vein endothelial cells (HUVECs), were treated with **M-BODIPY-GSH** for 30 minutes, the emission ratio was severely reduced, resulting in the ratio to be around 0.3. These results demonstrate the capability of **M-BODIPY-GSH** for differentiation ovarian cancer cells from normal cells. To verify that the obtained fluorescence signal indeed derived from GGT activity, inhibitor assay was performed. OVCAR5 cells were pretreated with various concentrations of acivicin, subsequently incubated with **M-BODIPY-GSH** for 30 minutes. After incubation, triggering of **M-BODIPY-GSH** by GGT was determined by monitoring the ratiometric fluorescence changes. As shown in Figure 3 and Figure S8, the ratio of the emissions from the yellow and red channels is dose-dependent. Increasing the concentration of acivicin from 0 to 20 μM induced a reduction of the fluorescence signal in the yellow channel and a marked enhancement of that in the red channel, resulting in a decreased ratio of 0.4. These imaging experiments are consistent with the specifically triggering **M-BODIPY-GSH** by GGT. For comparison, **C-BODIPY-GSH** gave intracellular turn-on fluorescence in the human ovarian cancer cells (Figure S9). The signals were greatly reduced when human ovarian cancer cells were pretreated with acivicin then loading with **C-BODIPY-GSH** (Figure S9). Collectively, these FIST probes are suitable for monitoring GGT activity in living cancer cells.

As shown in Scheme 1, the two probes are fluorophore-GSH adducts. The hydrophobic nature of the BODIPY unit attracts probes to the cell membrane and increases the effective probe–enzyme interactions. Consequently, **M-BODIPY-GSH** encounters GGT in transmembrane domains during the cellular uptake of the probe, which is involved in the cleavage of GSH to yield **BODIPY-Cys** with yellow fluorescence. **BODIPY-Cys** is sufficiently hydrophobic and

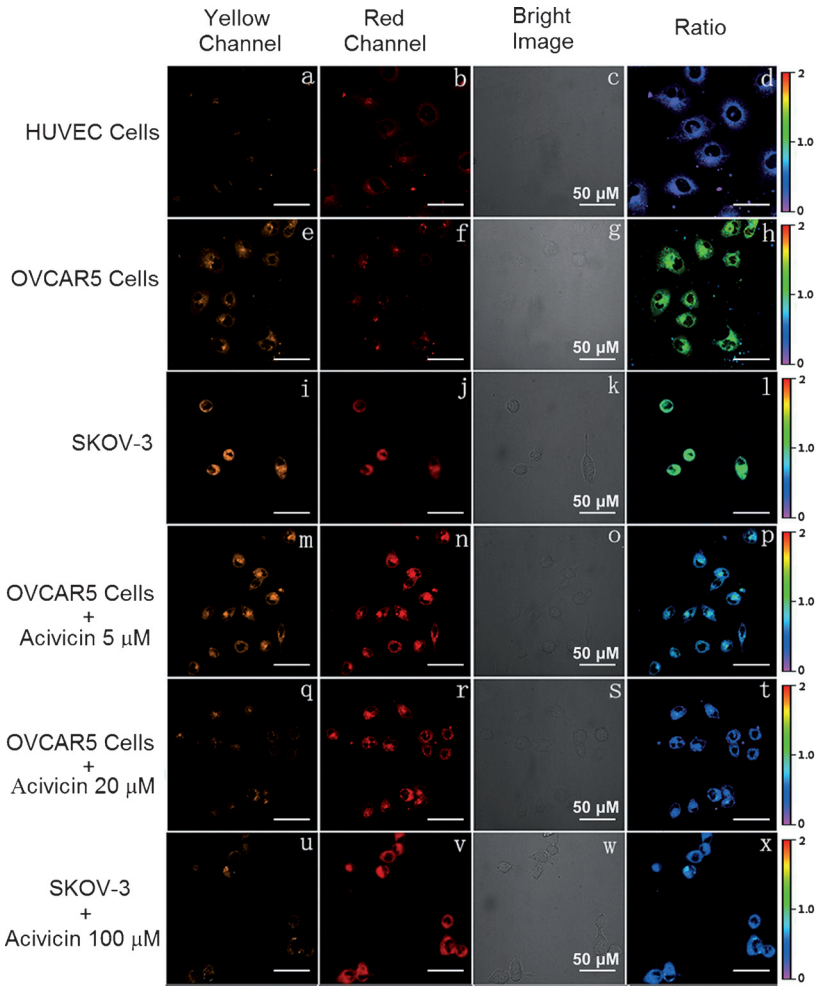

Figure 3. Fluorescent confocal image of normal cells (HUVEC) and cancer cells (OVCAR5, SKOV-3), the excitation wavelength was 514 nm and the emission was collected at 554–584 nm (yellow channel) and 595–635 nm (red channel), ratio image generated from yellow to red channel: a–d) HUVEC cells incubated with **M-BODIPY-GSH** (10 μm) for 30 minutes. e–h) OVCAR5 cells incubated with **M-BODIPY-GSH** (10 μm) for 30 minutes. i–l) SKOV-3 cells incubated with **M-BODIPY-GSH** (10 μm) for 30 minutes. m–t) OVCAR5 cells pretreated with acivicin for 30 minutes then loaded with **M-BODIPY-GSH** (10 μm) for 30 minutes. u–x) SKOV-3 cells pretreated with acivicin for 30 minutes then loaded with **M-BODIPY-GSH** (10 μm) for 30 minutes. The scale bar is 50 μm.

can be readily transported into cancer cells. This mechanism of visualizing GGT activity in living cells was revealed by co-localization experiments in both OVCAR5 and HUVEC cells. Such experiments were carried out using commercial available Lyso-Tracker Green, Mito-Tracker Green and Memb-Tracker Green, respectively. As shown in Figure S10, the yellow fluorescence from **BODIPY-Cys** co-localized well with these fluorescence signals from Lyso-Tracker Green and Mito-Tracker Green. In comparison, a poor overlap between **BODIPY-Cys** and Memb-Tracker Green was noted. Therefore, we infer that **BODIPY-Cys** is permeable to the cell membrane and distributes in cytoplasm with non-specific intracellular localization. For **M-BODIPY-GSH**, we also found that this probe exhibited cellular uptake into the cytoplasm of cells. In HUVEC cells, the intrinsic red fluorescence from **M-BODIPY-GSH** matched well with that of Lyso-Tracker Green and Mito-Tracker Green, suggesting that the probe distributed in both mitochondria and lysosomes. However, the co-localization assay in OVCAR5 cells showed that yellow fluorescence overlapped well with what observed with Lyso-Tracker Green and Mito-Tracker Green but not Memb-Tracker Green, which is consistent with that from **BODIPY-Cys**. Such co-staining pattern is attributed to variable GGT activity in different cells. Since GGT is over-expressed on the plasma membrane of OVCAR5, the incubation with **M-BODIPY-GSH** introduced the enzyme digestion in transmembrane domains to produce **BODIPY-Cys**, followed by the co-stain with commercial trackers. Taken together, **M-BODIPY-GSH** has proven to be a promising probe that specifically targets GGT in tumor cells, which undergoes an enzyme-mediated rapid and irreversible aromatic hydrocarbon transfer between the sulfur and nitrogen atoms to generate **BODIPY-Cys** in the cellular uptake, endowing dramatic fluorescence imaging variations.

In summary, we report the design of two new GGT-specific FIST probes for monitoring the GGT activity. Upon GGT enzymatic cleavage of γ-glutamyl linkage, the released amino group in cysteinyl-glycine residue undergoes intramolecular rearrangement to yield amino-substituted BODIPY. This aromatic hydrocarbon transfer between the sulfur and nitrogen atoms happens through five-membered cyclic transition state. Such a translation induces dramatic photophysical responses to the GGT activity. Importantly, these FIST probes can differentiate ovarian cancer cells from normal cells via living-cell imaging of GGT. In light of their capability for specific monitoring the GGT activity in cancer cells, we expect they will function as imaging probes in vivo. We also expect that the design strategy using enzyme-mediated aromatic hydrocarbon transfer between the sulfur and nitrogen atoms would be generalizable for developing a wide range of activatable probes.

Keywords: aromatic hydrocarbon transfer · enzymes · fluorescence · photophysics · tumor cells

How to cite: *Angew. Chem. Int. Ed.* **2015**, *54*, 7349–7353
Angew. Chem. **2015**, *127*, 7457–7461

[1] G. Blum, G. von Degenfeld, M. J. Merchant, H. M. Blau, M. Bogyo, *Nat. Chem. Biol.* **2007**, *3*, 668.
[2] C. Bremer, C.-H. Tung, R. Weissleder, *Nat. Med.* **2001**, *7*, 743.
[3] J. W. Chang, R. E. Moellering, B. F. Cravatt, *Angew. Chem. Int. Ed.* **2012**, *51*, 966; *Angew. Chem.* **2012**, *124*, 990.

[4] T. Myochin, K. Hanaoka, T. Komatsu, T. Terai, T. Nagano, *J. Am. Chem. Soc.* **2012**, *134*, 13730.
[5] S. Mizukami, R. Takikawa, F. Sugihara, M. Shirakawa, K. Kikuchi, *Angew. Chem. Int. Ed.* **2009**, *48*, 3641; *Angew. Chem.* **2009**, *121*, 3695.
[6] Y. Fujikawa, Y. Urano, T. Komatsu, K. Hanaoka, H. Kojima, T. Terai, H. Inoue, T. Nagano, *J. Am. Chem. Soc.* **2008**, *130*, 14533.
[7] R. Baba, Y. Hori, S. Mizukami, K. Kikuchi, *J. Am. Chem. Soc.* **2012**, *134*, 14310.
[8] H. Shi, R. T. K. Kwok, J. Liu, B. Xing, B. Z. Tang, B. Liu, *J. Am. Chem. Soc.* **2012**, *134*, 17972.
[9] J. Rao, C. Hottinger, A. Khan, *J. Am. Chem. Soc.* **2014**, *136*, 5872.
[10] H. X. Xie, J. Mire, Y. Kong, M. H. Chang, H. A. Hassaounah, C. N. Thornton, J. C. Sacchettini, J. D. Cirillo, J. Rao, *Nat. Chem.* **2012**, *4*, 802.
[11] Y. Kong, H. Ao, Y. H. Ren, S. Subbian, S. L. G. Cirillo, J. C. Sacchettini, J. Rao, J. D. Cirillo, *Proc. Natl. Acad. Sci. USA* **2010**, *107*, 12239.
[12] D. Ye, G. Liang, M. L. Ma, J. Rao, *Angew. Chem. Int. Ed.* **2011**, *50*, 2275; *Angew. Chem.* **2011**, *123*, 2323.
[13] L. Li, J. Ge, H. Wu, Q.-H. Xu, S. Q. Yao, *J. Am. Chem. Soc.* **2012**, *134*, 12157.
[14] A. Östman, C. Hellberg, F. D. Böhmer, *Nat. Rev. Cancer* **2006**, *6*, 307.
[15] A. Razgulin, N. Ma, J. Rao, *Chem. Soc. Rev.* **2011**, *40*, 4186.
[16] Y. Urano, M. Sakabe, N. Kosaka, M. Ogawa, M. Mitsunaga, D. Asanuma, M. Kamiya, M. R. Young, T. Nagano, P. L. Choyke, *Sci. Transl. Med.* **2011**, *3*, 110ra119.
[17] M. Kamiya, H. Kobayashi, Y. Hama, Y. Koyama, M. Bernardo, T. Nagano, P. L. Choyke, Y. Urano, *J. Am. Chem. Soc.* **2007**, *129*, 3918.
[18] H. Zhang, J. Fan, J. Wang, B. Dou, F. Zhou, J. Cao, J. Qu, Z. Cao, W. Zhao, X. Peng, *J. Am. Chem. Soc.* **2013**, *135*, 17469.
[19] S. Gehrig, M. A. Mall, C. Schultz, *Angew. Chem. Int. Ed.* **2012**, *51*, 6258; *Angew. Chem.* **2012**, *124*, 6363.
[20] W. C. Silvers, B. Prasai, D. H. Burk, M. L. Brown, R. L. McCarley, *J. Am. Chem. Soc.* **2013**, *135*, 309.
[21] S. U. Hettiarachchi, B. Prasai, R. L. McCarley, *J. Am. Chem. Soc.* **2014**, *136*, 7575.
[22] H. Zhang, J. Fan, J. Wang, S. Zhang, B. Dou, X. Peng, *J. Am. Chem. Soc.* **2013**, *135*, 11663.
[23] M. Sakabe, D. Asanuma, M. Kamiya, R. J. Iwatate, K. Hanaoka, T. Terai, T. Nagano, Y. Urano, *J. Am. Chem. Soc.* **2013**, *135*, 409.
[24] M. H. Hanigan, W. A. Ricketts, *Biochemistry* **1993**, *32*, 6302.
[25] A. Pompella, V. De Tata, A. Paolicchi, F. Zunino, *Biochem. Pharmacol.* **2006**, *71*, 231.
[26] M. H. Hanigan, H. F. Frierson Jr., J. E. Brown, M. A. Lovell, P. T. Taylor, *Cancer Res.* **1994**, *54*, 286.
[27] D. Yao, D. Jiang, Z. Huang, J. Lu, Q. Tao, Z. Yu, X. Meng, *Cancer* **2000**, *88*, 761.
[28] F. Schiele, Y. Artur, D. Bagrel, C. Petitclerc, G. Siest, *Clin. Chim. Acta* **1981**, *112*, 187.
[29] E. Prusak, M. Siewinski, A. Szewczuk, *Clin. Chim. Acta* **1980**, *107*, 21.
[30] X. Wang, J. Cao, C. Zhao, *Org. Biomol. Chem.* **2012**, *10*, 4689.
[31] L. Han, J. Hiratake, A. Kamiyama, K. Sakata, *Biochemistry* **2007**, *46*, 1432.
[32] L.-Y. Niu, Y.-S. Guan, Y.-Z. Chen, L.-Z. Wu, C.-H. Tung, Q.-Z. Yang, *J. Am. Chem. Soc.* **2012**, *134*, 18928.
[33] F. Wang, Z. Guo, X. Li, X. Li, C. Zhao, *Chem. Eur. J.* **2014**, *20*, 11471.

Received: March 30, 2015
Published online: May 4, 2015

